Gravitational Lensing

See the same effects that occur in more familiar optical circumstances: magnification and distortion (shear)

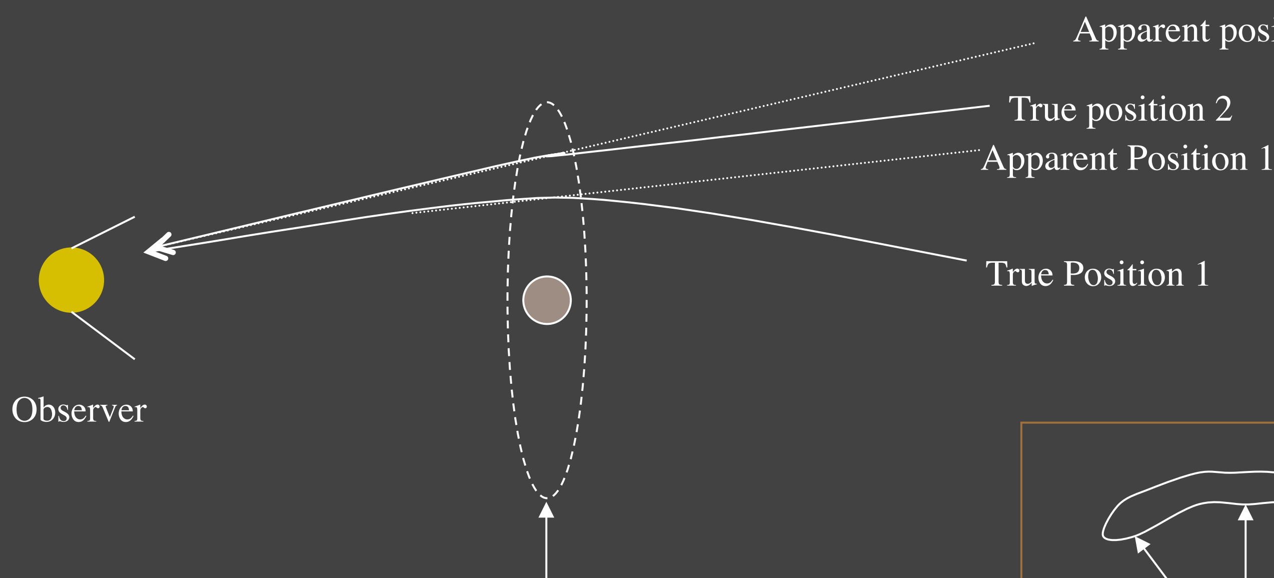

Objects farther from the line of sight are distorted less.

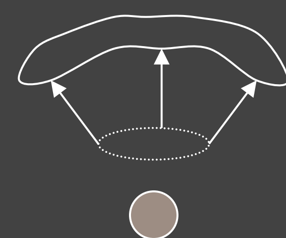

“Looking into” the lens: extended objects are tangentially distorted...

Lensing conserves surface brightness: bigger image ←→ magnified

Gravitational Lensing by Clusters

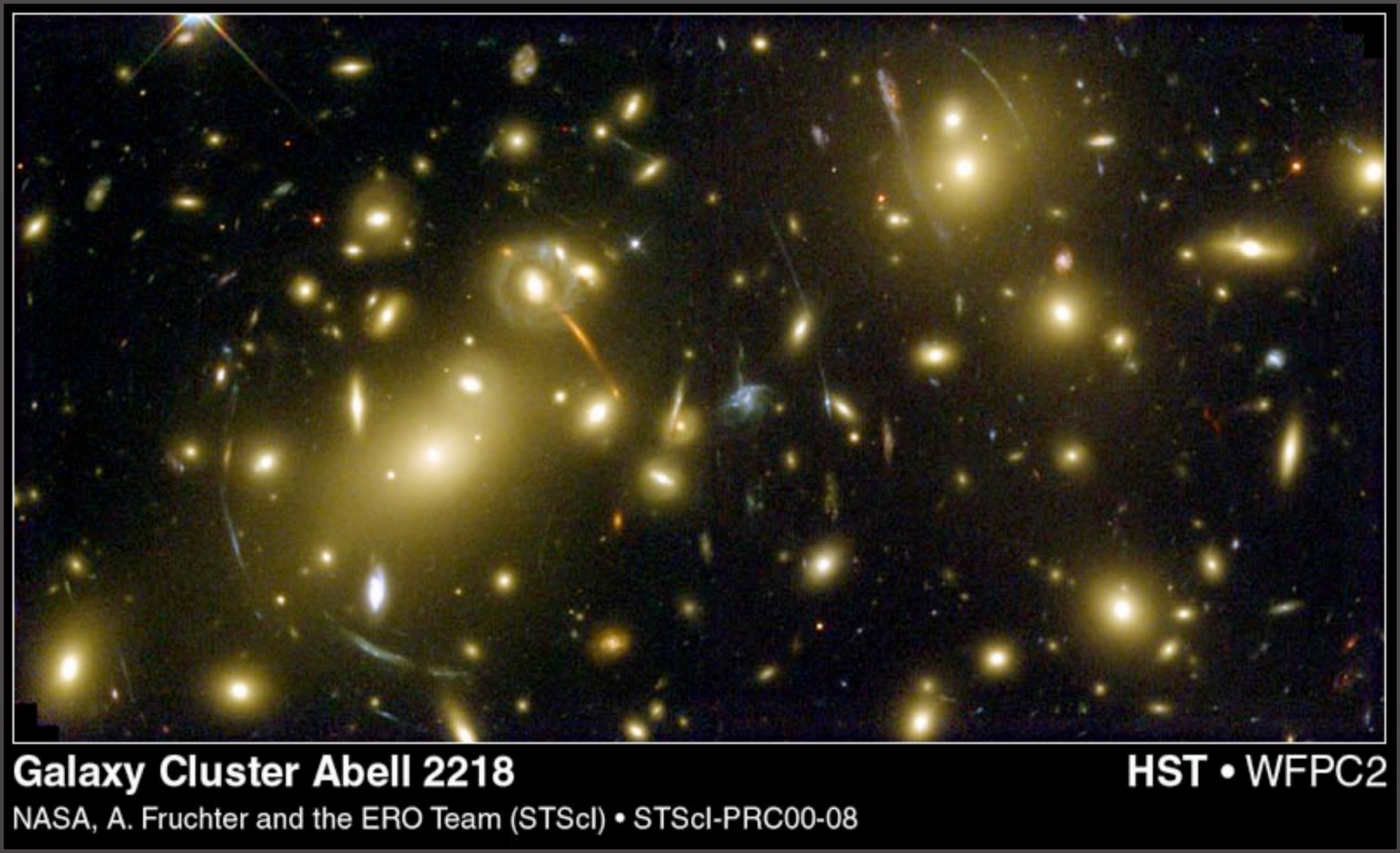

Strong Lensing

Deep images: WL reconstrution of Cluster Mass Profile

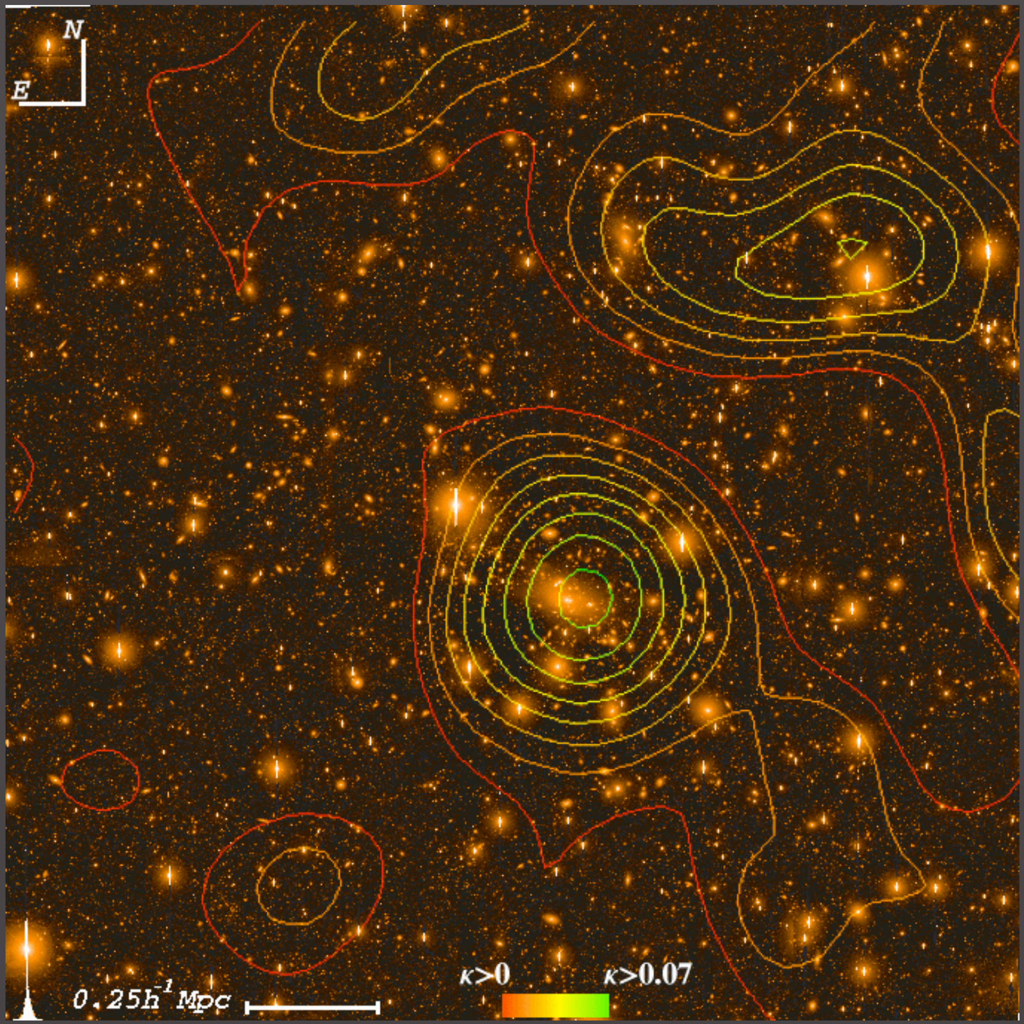

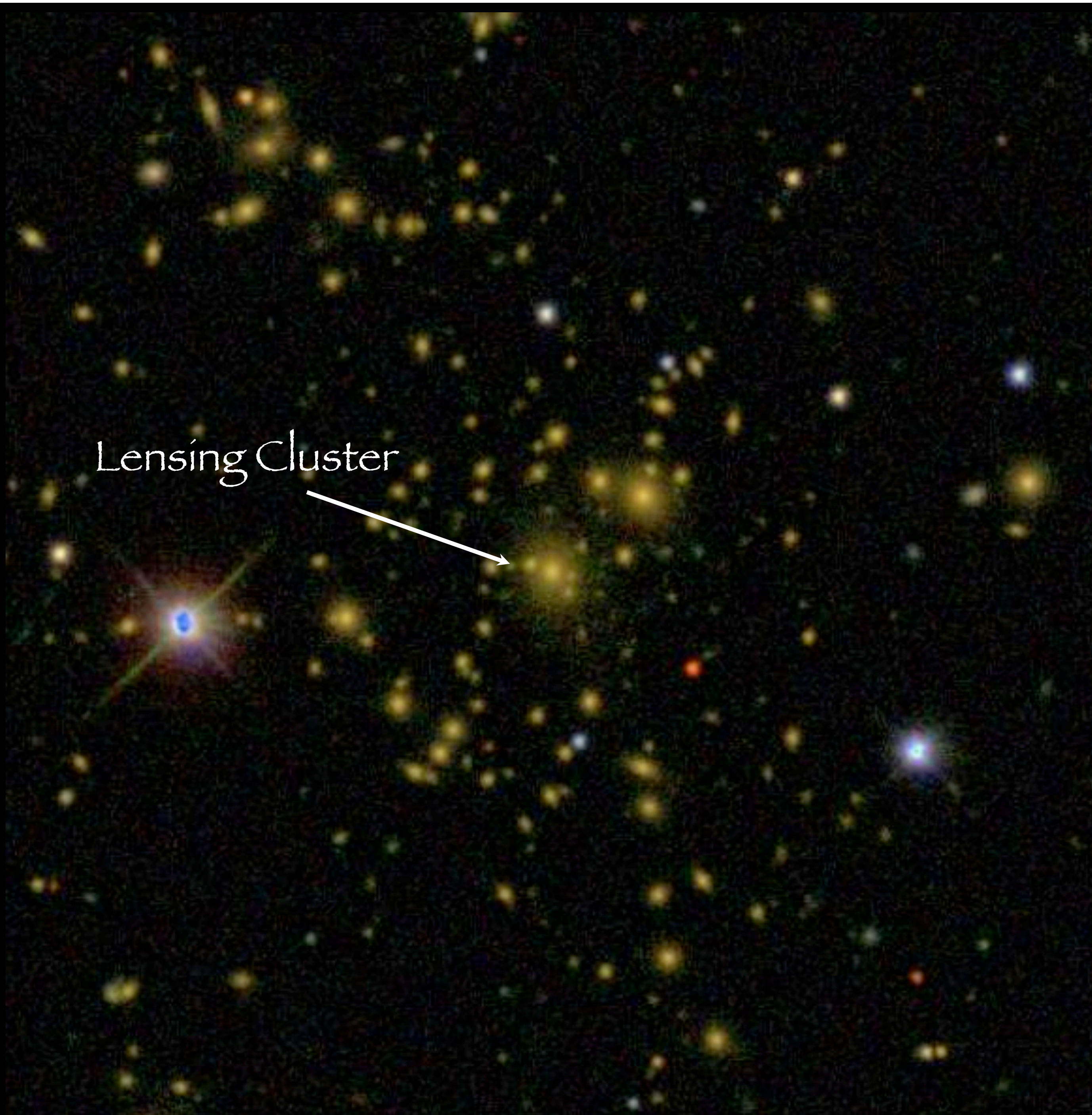
Lensing Cluster

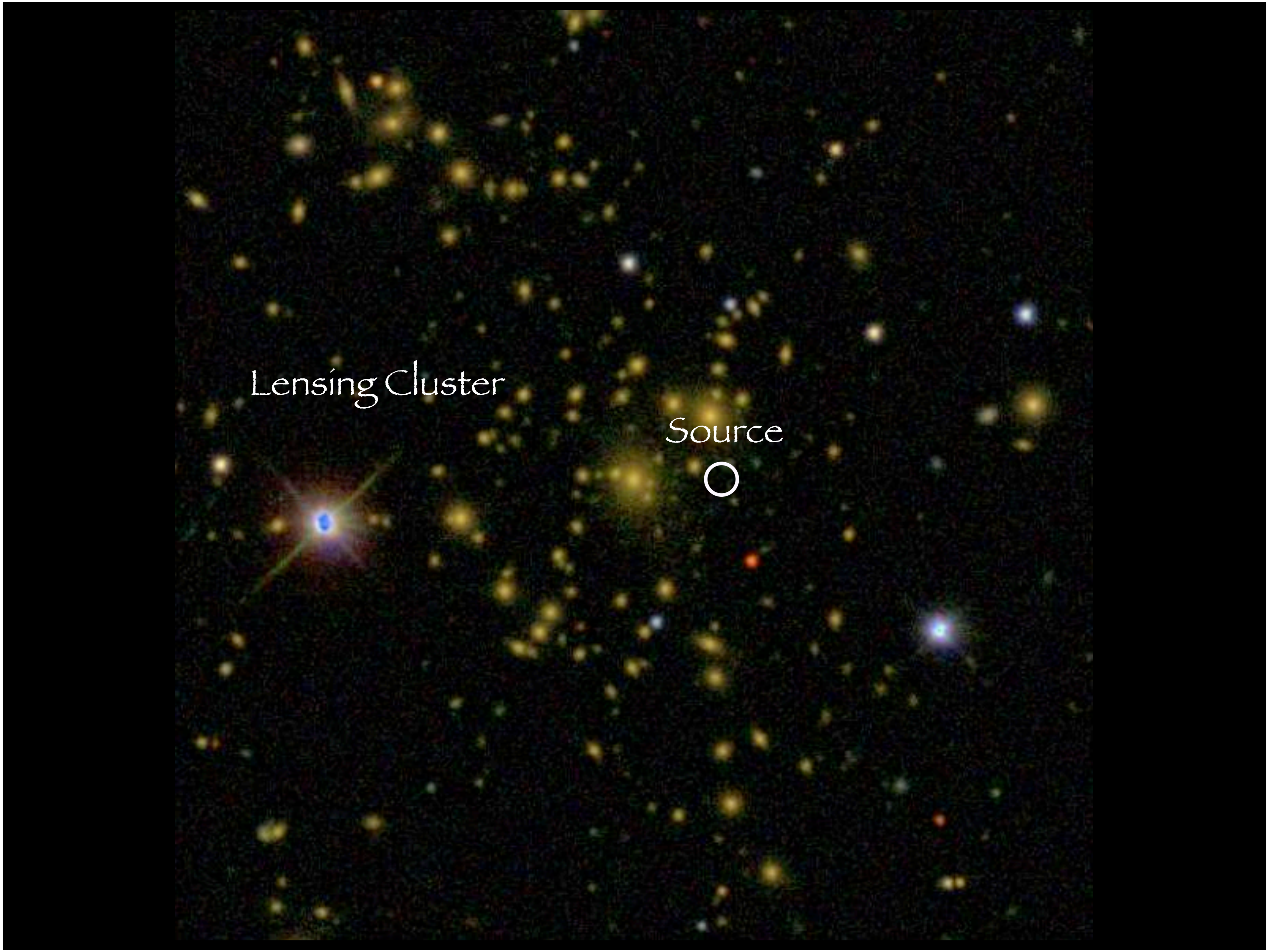
Lensing Cluster
Source

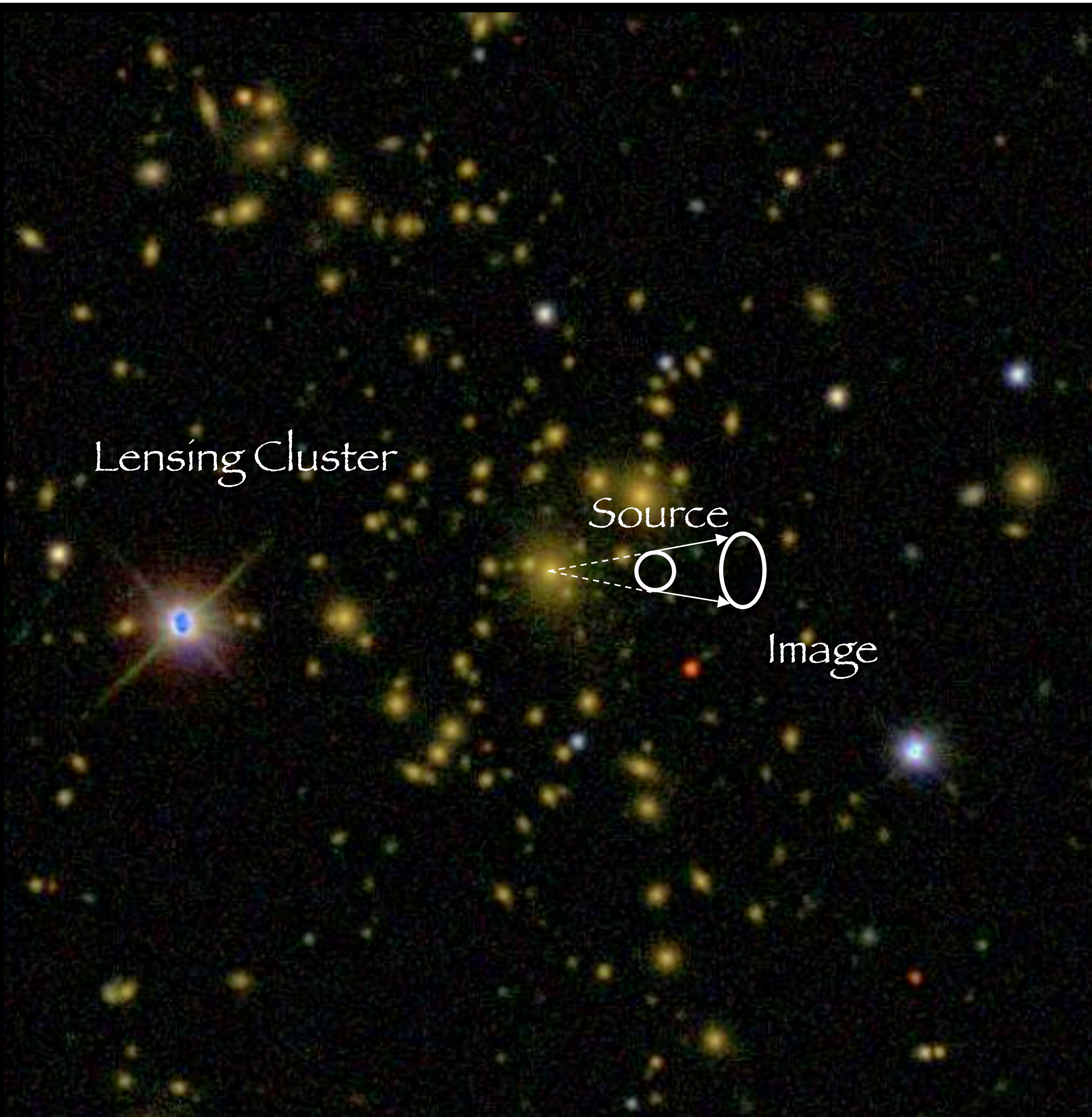
Lensing Cluster
Source
Image

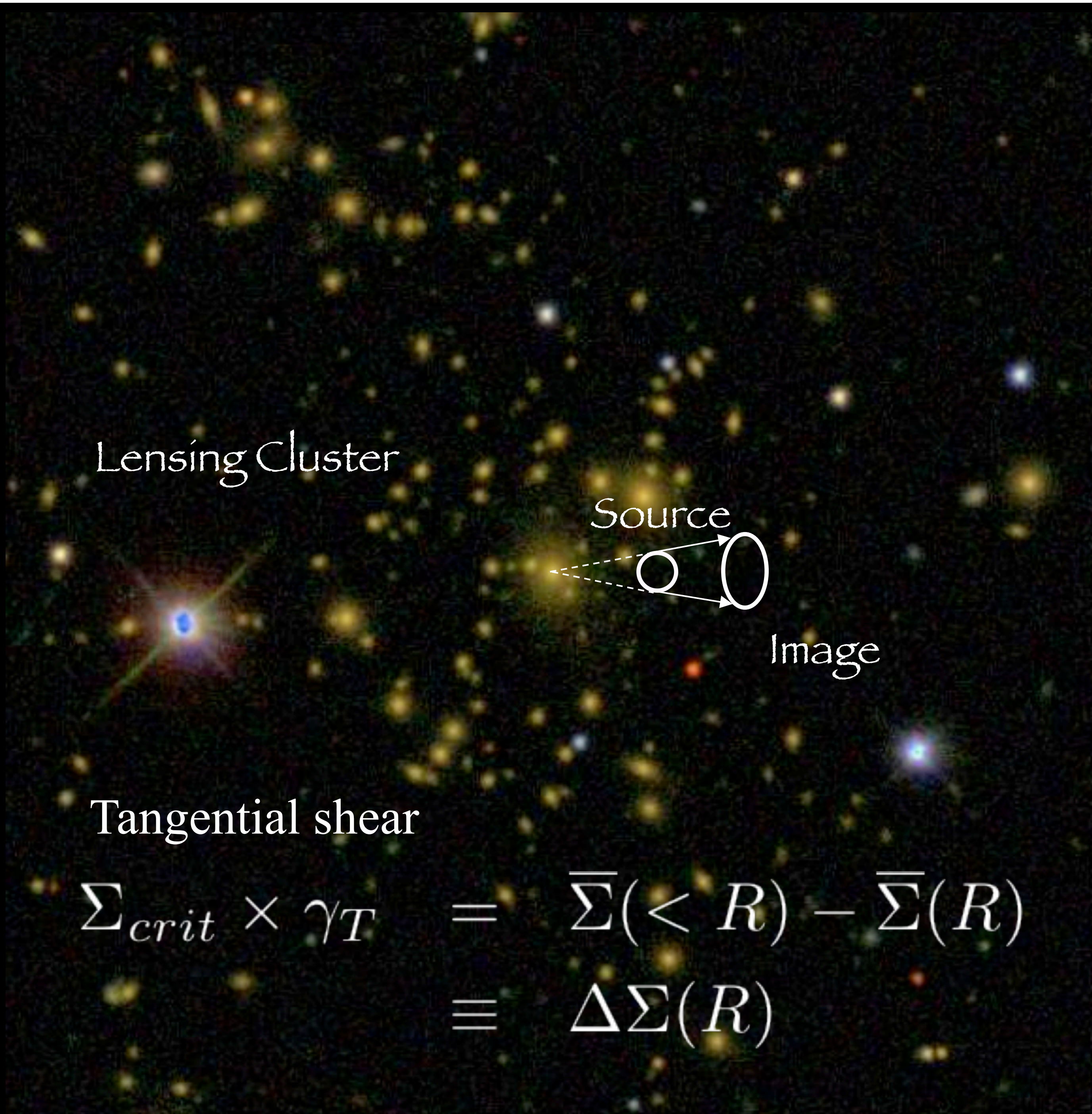
Lensing Cluster
Source
Image
Tangential shear
$$\Sigma_{crit} \times \gamma_T = \bar{\Sigma}(< R) - \bar{\Sigma}(R)$$
$$\equiv \Delta\Sigma(R)$$

Statistical Weak Lensing by Galaxy Clusters

Mean Tangential Shear Profile in Optical Richness (N_{gal}) Bins to 30 h^{-1}Mpc

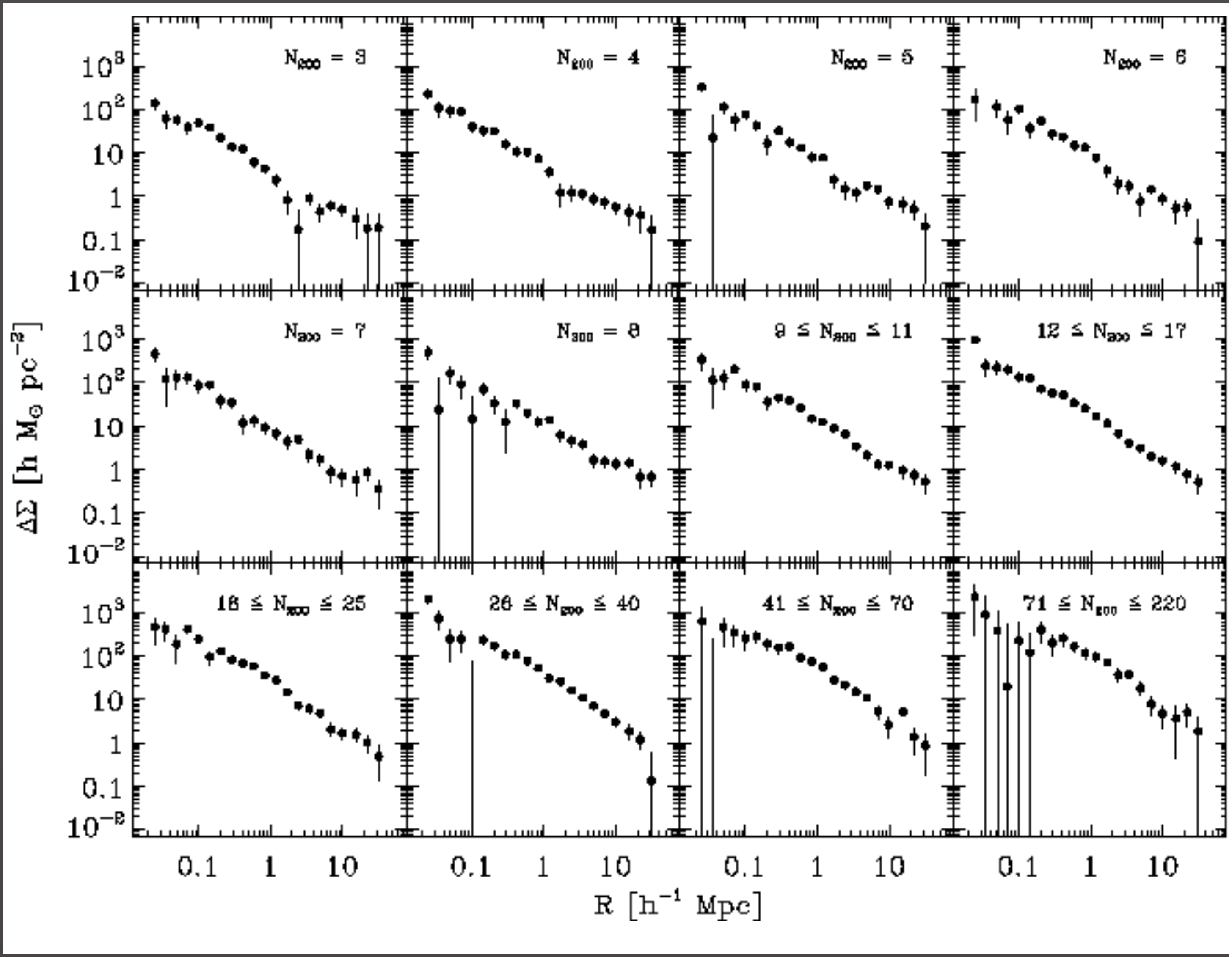

Sheldon, Johnston, etal SDSS

Statistical Weak Lensing by Galaxy Clusters

Mean Tangential Shear Profile in Optical Richness (N_{gal}) Bins to 30 h^{-1}Mpc

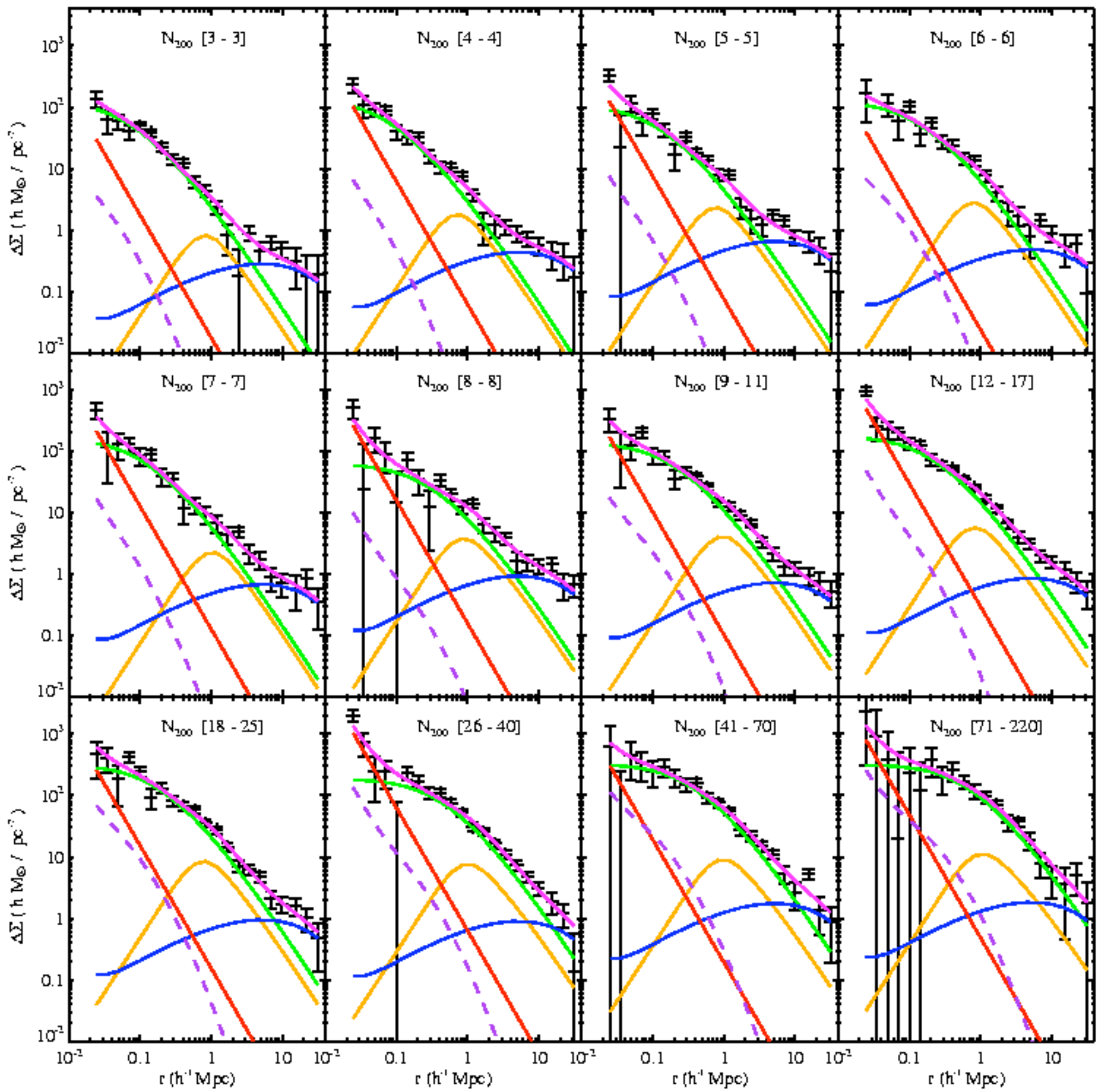

Johnston, Sheldon, etal SDSS

Mean 3D Cluster Mass Profile

from Statistical Lensing

Johnston, etal

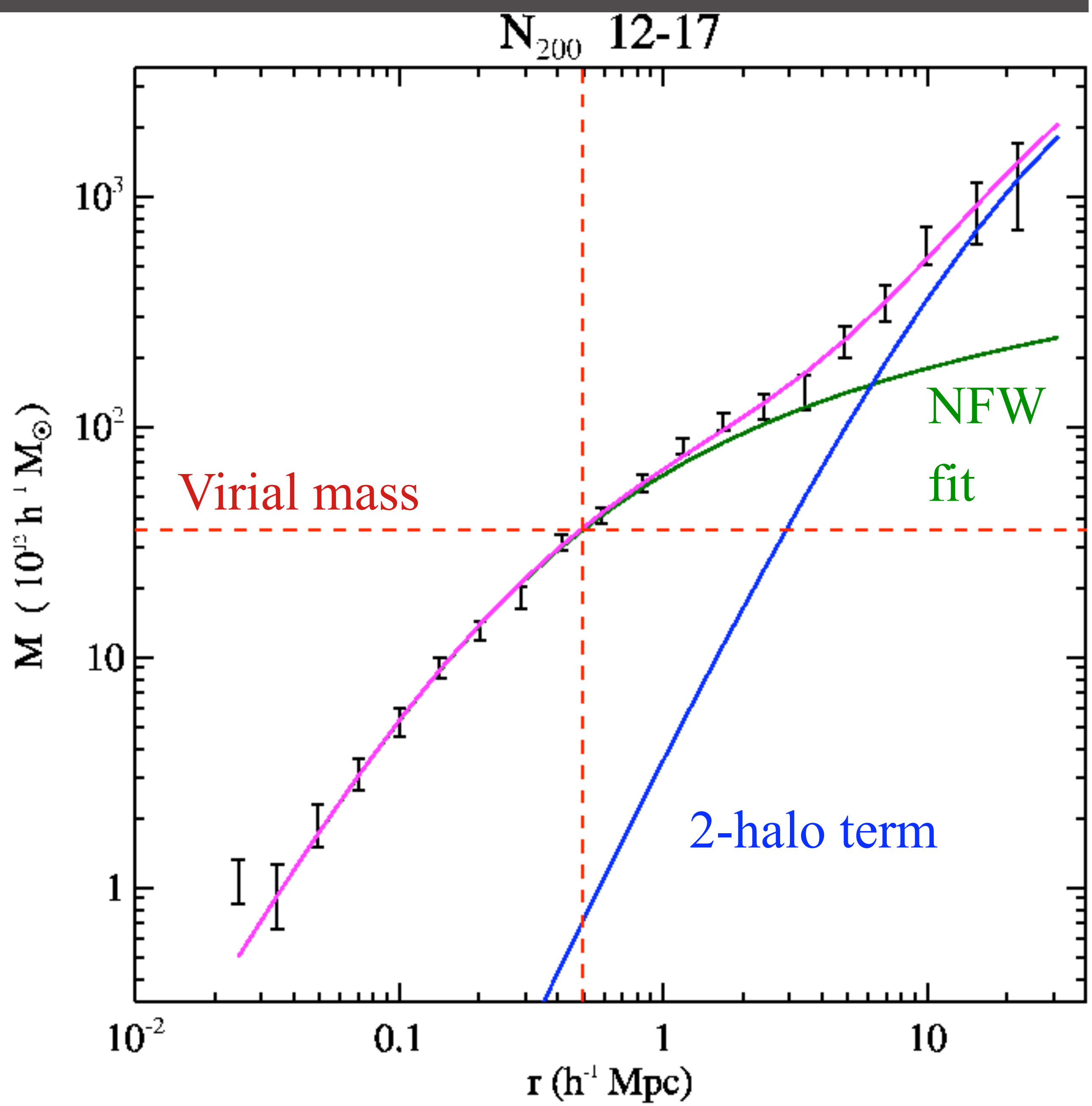

Statistical Weak Lensing Calibrates Cluster Mass vs. Observable Relation

Cluster Mass vs. Number of galaxies they contain

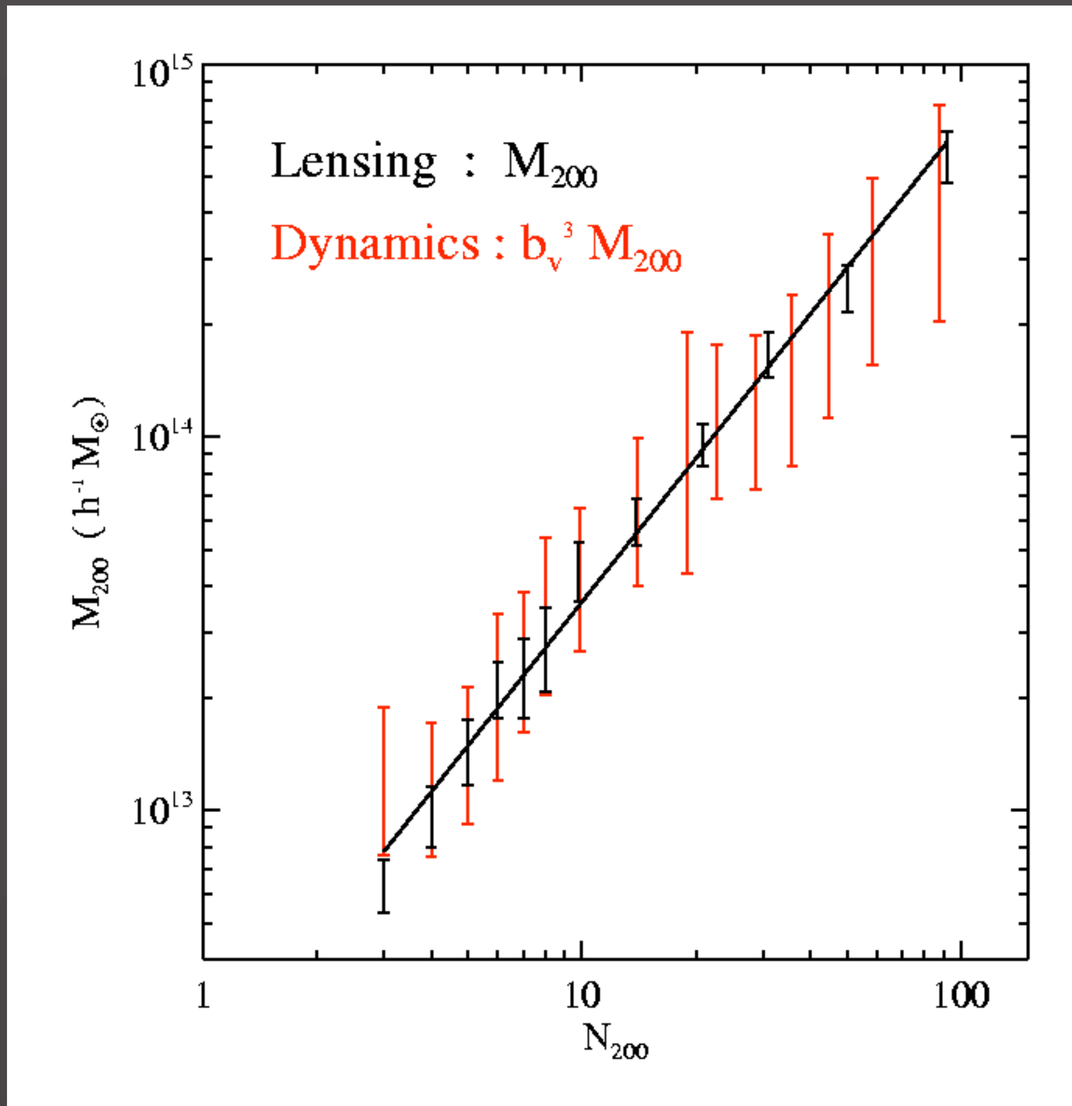

Statistical Lensing eliminates projection effects of individual cluster mass Estimates

~50% scatter in mass vs optical richness

Future:
use this to independently calibrate, e.g., SZE vs. Mass

Johnston, Sheldon, etal

Weak Lensing: Cosmic Shear

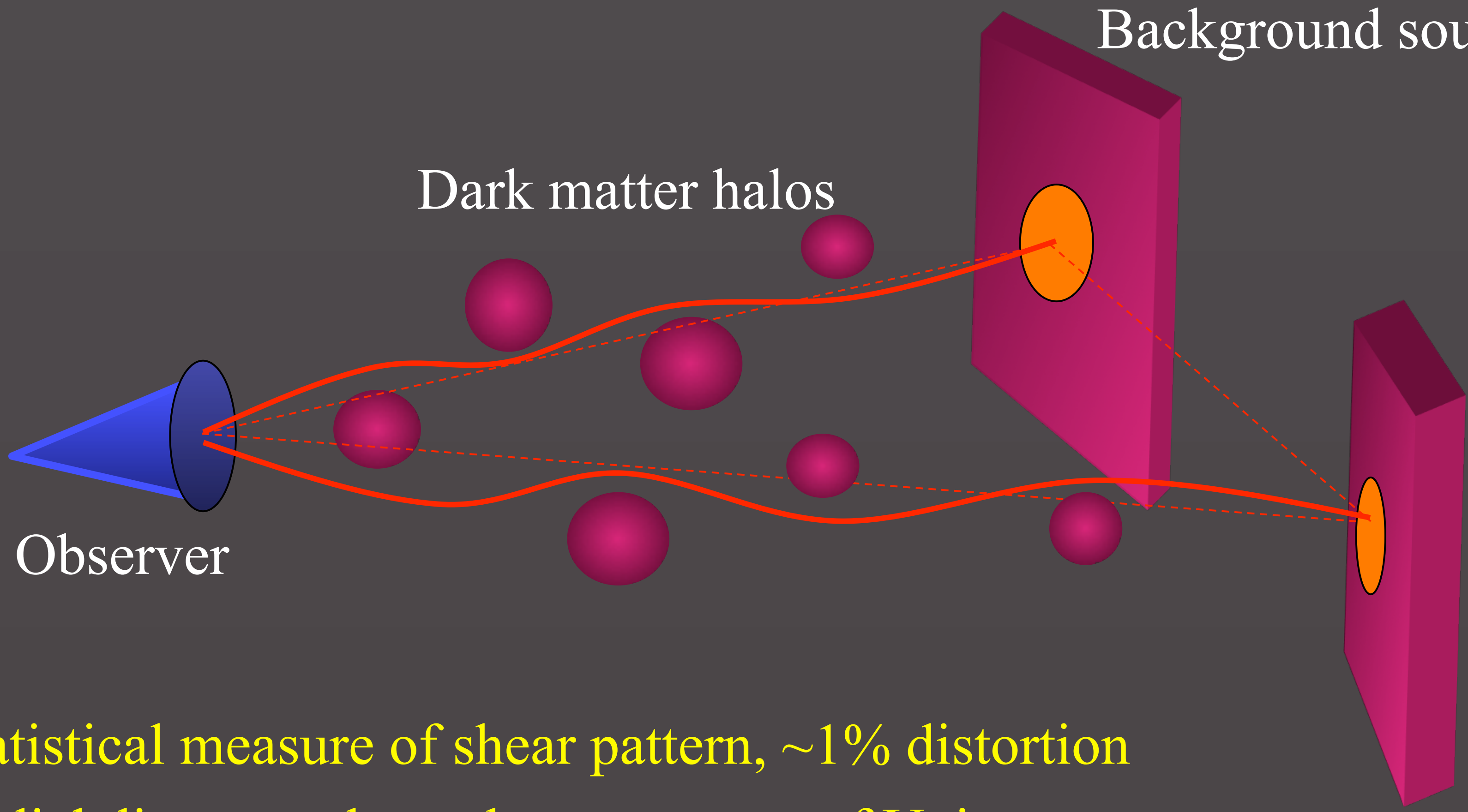

- Statistical measure of shear pattern, ~1% distortion
- Radial distances depend on *geometry* of Universe
- Foreground mass distribution depends on *growth* of structure

Gravitational Lensing

- A simple scattering experiment:

$$ds^2 = -(1+2\Phi)dt^2 + a^2(t)(1-2\Phi)dr_i dr^i$$

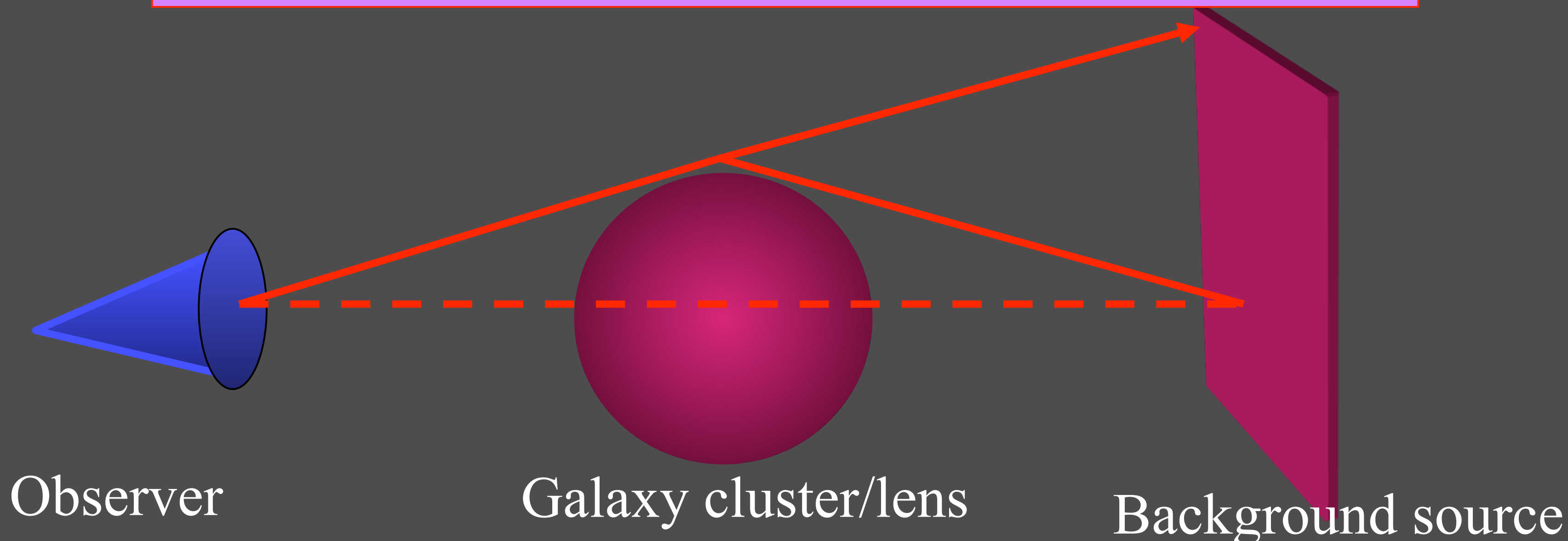

Gravitational Lensing

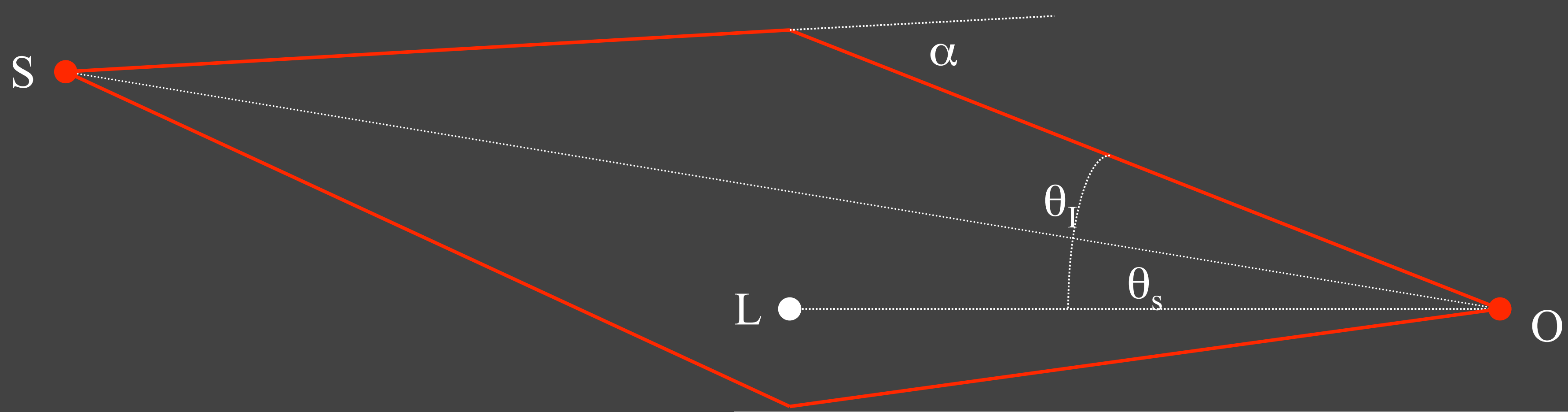

Lens equation: $\vec{\theta}_S = \vec{\theta}_I - \frac{D^A_{LS}}{D^A_{OS}}\vec{\alpha}\ , \quad \vec{\alpha} = \nabla\Psi, \quad \nabla^2\Psi = 2\frac{\Sigma}{\Sigma_{crit}} \equiv 2\kappa$

Amplification Matrix:

$$\frac{\partial\theta^i_S}{\partial\theta^j_I} = A_{ij} = \begin{pmatrix} 1-\kappa-\gamma_1 & -\gamma_2 \\ -\gamma_2 & 1-\kappa+\gamma_1 \end{pmatrix}$$

$$\gamma_1 = \partial^2\Psi/\partial\theta_1^2 - \partial^2\Psi/\partial\theta_2^2\ , \quad \gamma_2 = \partial_{12}\Psi$$

Amplification: $A = (\det A_{ij})^{-1}$

Shear: $\gamma = (\gamma_1^2 + \gamma_2^2)^{1/2}$

The deflection α is sensitive to *all* mass, luminous or dark. Thus, lensing probes the dark matter halos of distant galaxies and clusters.

Distance dependence of lensing observations

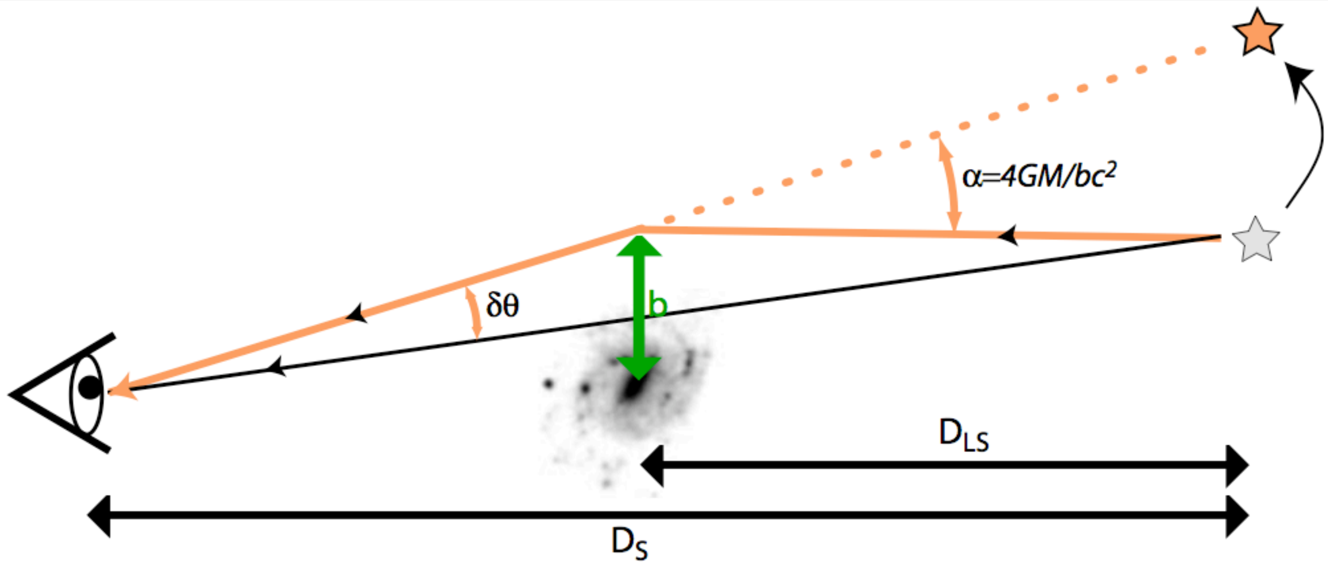

$$\delta\theta = \frac{4GM}{bc^2}\,\frac{D_{LS}}{D_S}$$

Lensing measures the *projected* potential of mass along the line of sight, with a weighting for geometric distance factors:

$$\psi_l = \int_{\mathrm{lens}} d\chi\, \nabla_\perp^2 (\Phi + \Psi)$$

$$\kappa_s = A_{ls}\psi_l/(2a_l D_l)$$

$$A_{ls} \equiv \frac{D_{ls}}{D_s} \approx (1 - D_l/D_s)(1 - \omega_k D_l D_s/2) \quad z_s > z_l$$

Weak gravitational lensing

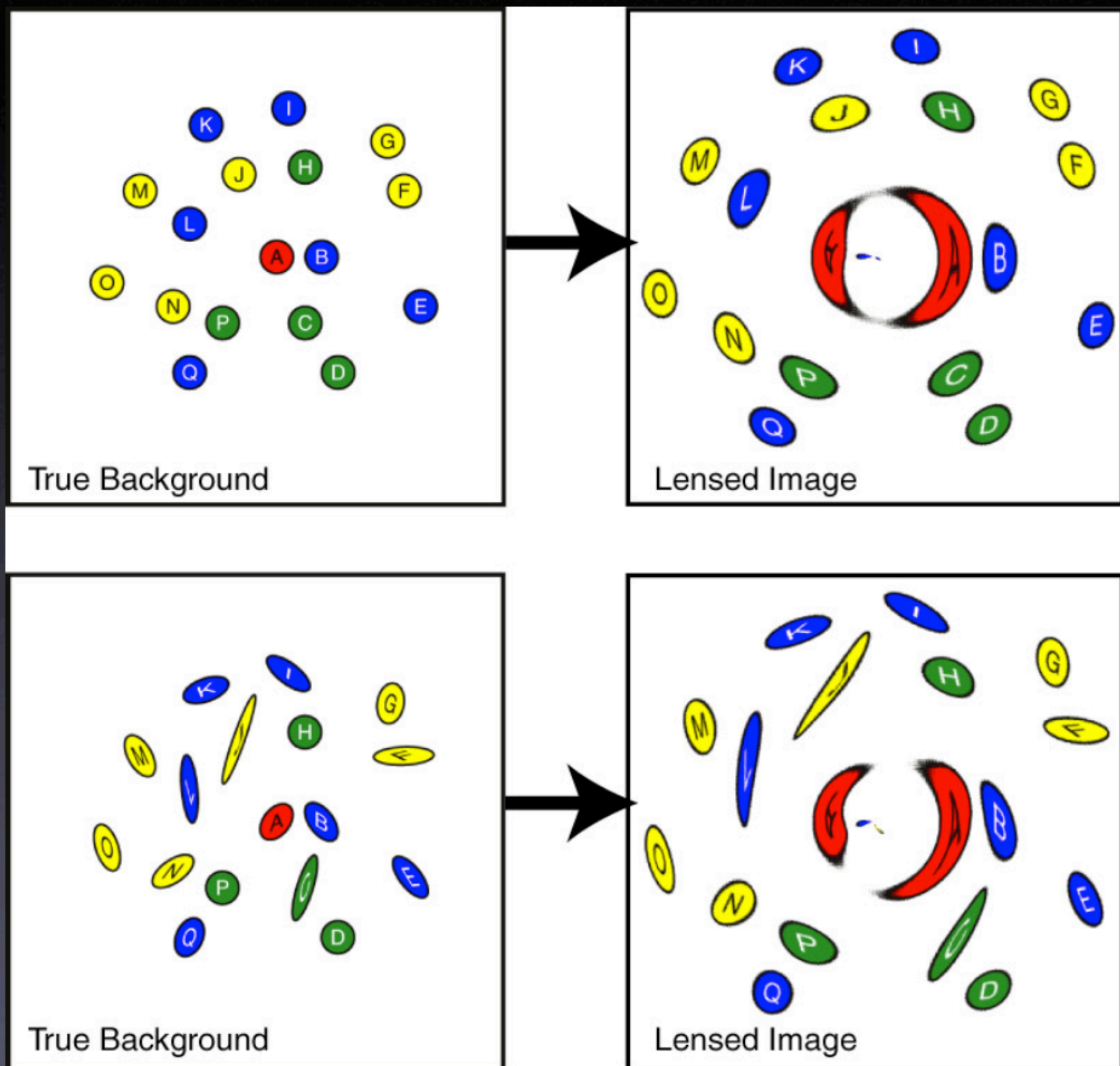

- Deflection angles are not generally observable since lensing mass cannot be removed!
- In weak gravitational lensing, we instead measure the gradients of the deflection angle as distortions to the shapes of galaxies.
- The intrinsic variation of galaxy shapes then becomes a source of noise which averages away as $\sqrt{N}$
- Cosmic signal is ~0.02; shape noise is $0.25/\sqrt{N}$; N~1e9!

Weak lensing: shear and mass

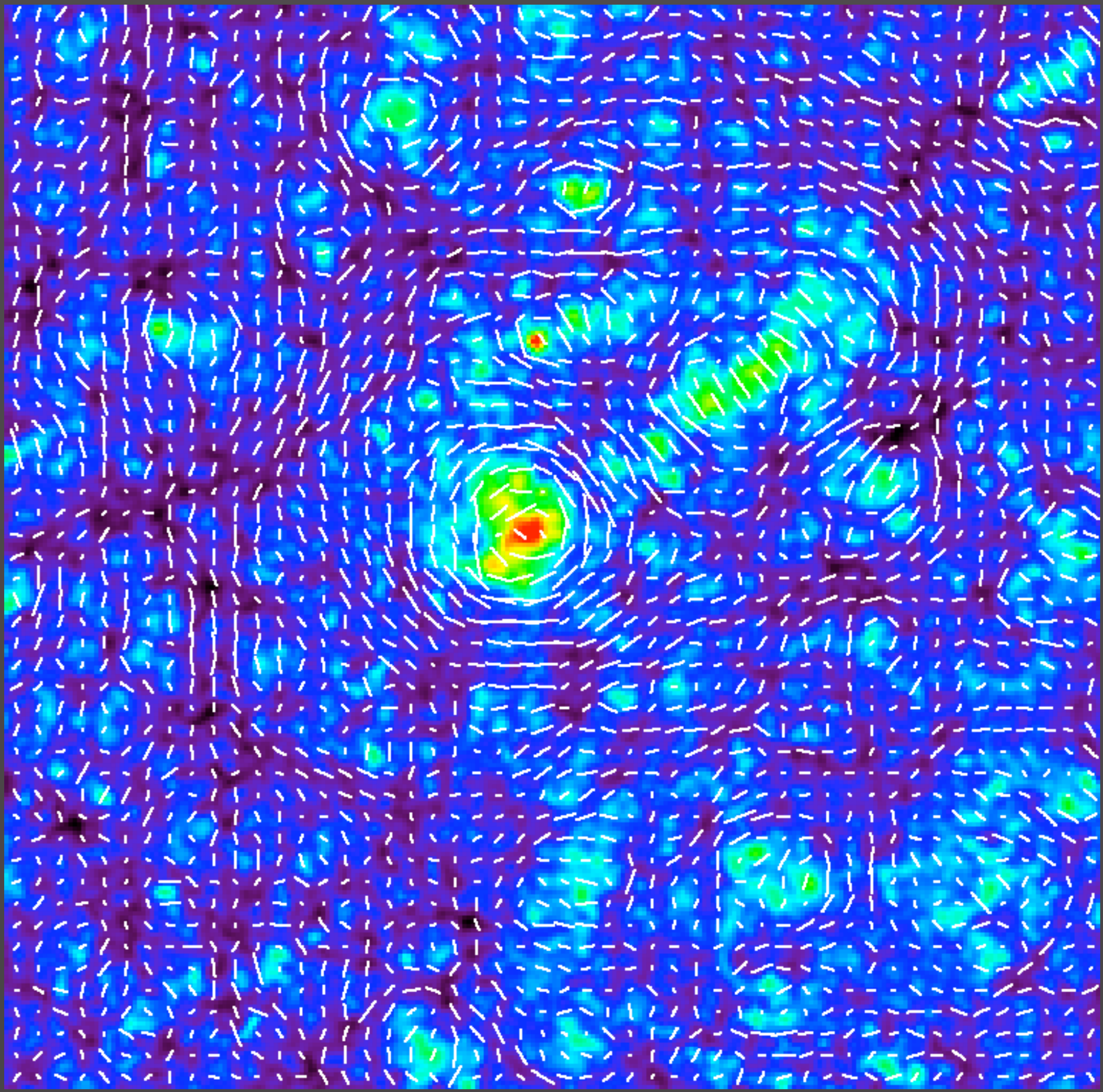

Reducing WL Shear Systematics

Cosmic Shear

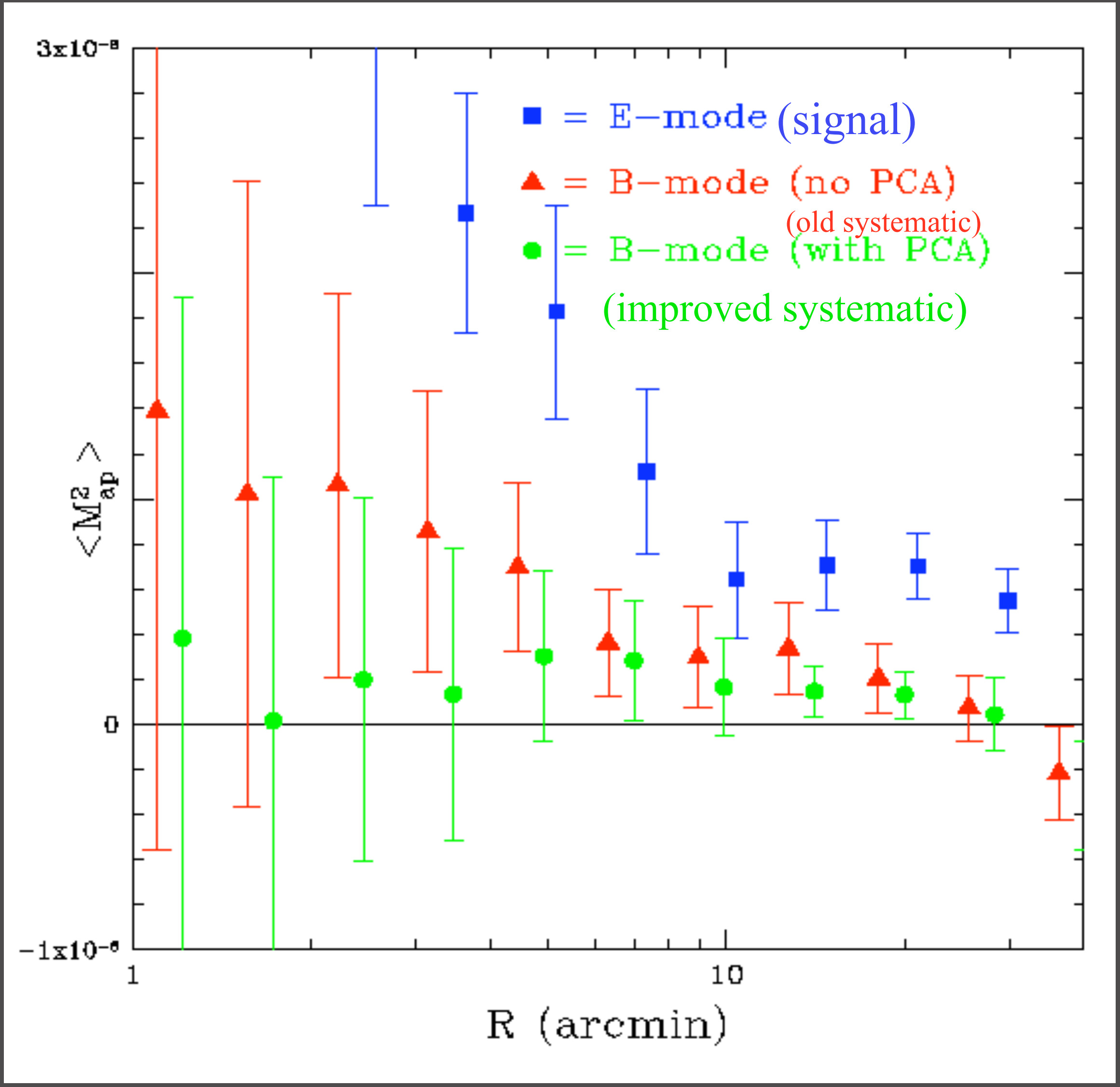

Results from
75 sq. deg. WL
Survey with
Mosaic II and BTC
on the Blanco 4-m
Jarvis, etal

Science Results: CFH Legacy Survey

- Completed 140 sq deg of ugriz imaging.
- Fu et al (2008): results from i-band in 57 deg^2
- Uses 1-sq-degree Megacam on CFH 3.5m

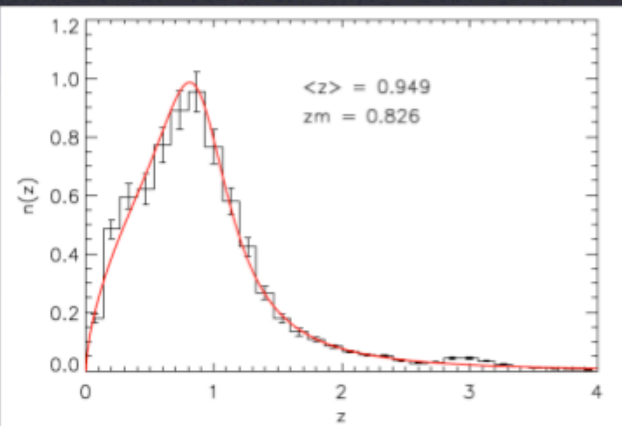

Fig. 9. Final normalised redshift distribution. Galaxies are selected in the range [0;4], and the best-fit is given for function given in Eq. (14). Note that the fit is only performed in the interval [0;2.5].

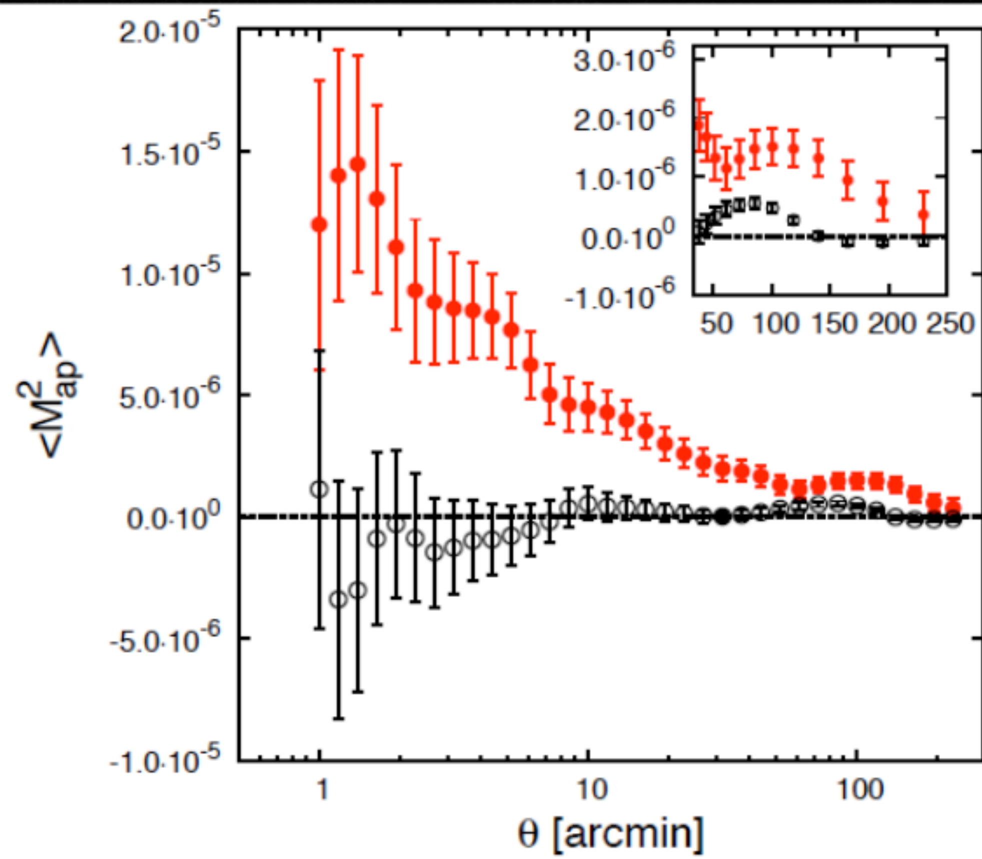

Fig. 4. Two-point statistics from the combined 57 pointings. The error bars of the E-mode include statistical noise added in quadrature to the non-Gaussian cosmic variance. Only statistical uncertainty contributes to the error budget for the B-mode. Red filled points show the E-mode, black open points the B-mode. The enlargements in each panel show the signal in the angular range 35′-230′.

Lensing Tomography

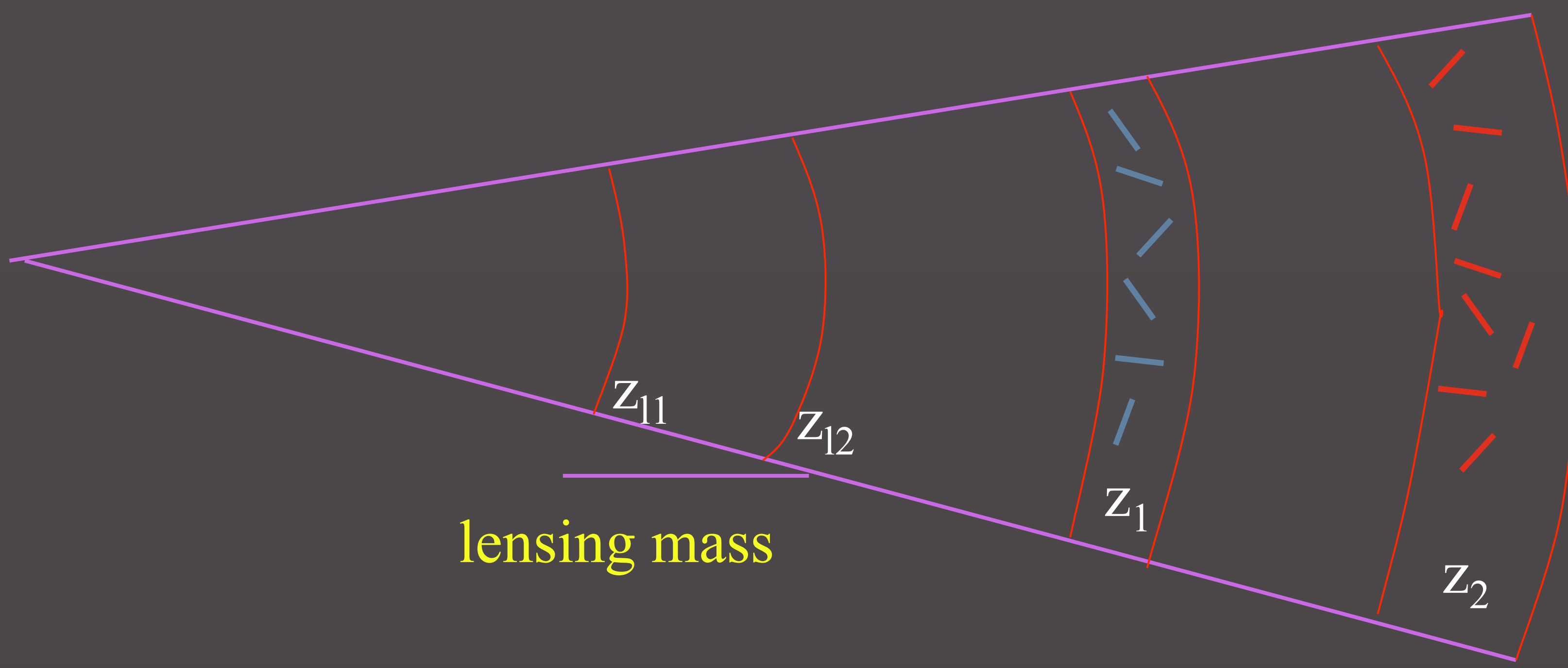

Shear at z_1 and z_2 given by integral of growth function & distances over lensing mass distribution.

Weak Lensing Tomography

- Shear-shear & galaxy-shear correlations probe distances & growth rate of perturbations

$$C_\ell^{x_a x_b} = \int dz \frac{H(z)}{D_A^2(z)} W_a(z) W_b(z) P^{s_a s_b}(k = \ell / D_A; z)$$

- Galaxy correlations determine galaxy bias priors
- Statistical errors on shear-shear correlations:

$$\Delta C_\ell = \sqrt{\frac{2}{(2\ell + 1) f_{sky}}} \left(C_\ell + \frac{\sigma^2(\gamma_i)}{n_{eff}} \right)$$

- Requirements: Sky area, depth, photo-z's, image quality & <u>stability</u>

Weak Lensing Tomography: DES

DARK ENERGY SURVEY

- Cosmic Shear Angular Power Spectrum in Photo-z Slices

- Shapes of ~300 million well-resolved galaxies, $\langle z \rangle = 0.7$

- Primary Systematics: photo-z's, PSF anisotropy, shear calibration

- Extra info in bispectrum & galaxy-shear: robust

Huterer etal

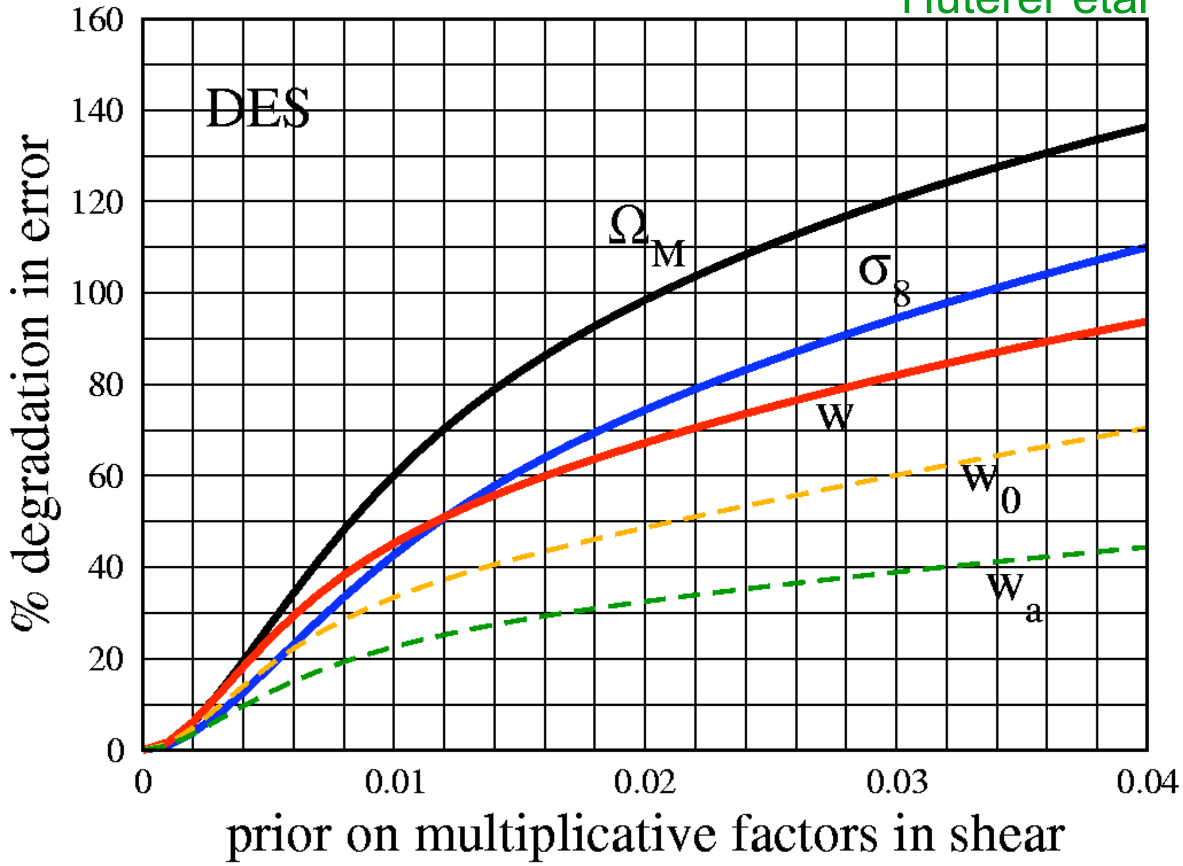

$$C_\ell^{x_a x_b} = \int dz \frac{H(z)}{D_A^2(z)} W_a(z) W_b(z) P^{s_a s_b}(k = \ell / D_A; z)$$

$$\Delta C_\ell = \sqrt{\frac{2}{(2\ell+1) f_{sky}}} \left(C_\ell + \frac{\sigma^2(\gamma_i)}{n_{eff}} \right)$$

Theory Uncertainty in *P(k)* and WL

Residual of the shear convergence power spectrum relative to simulation with dark matter only

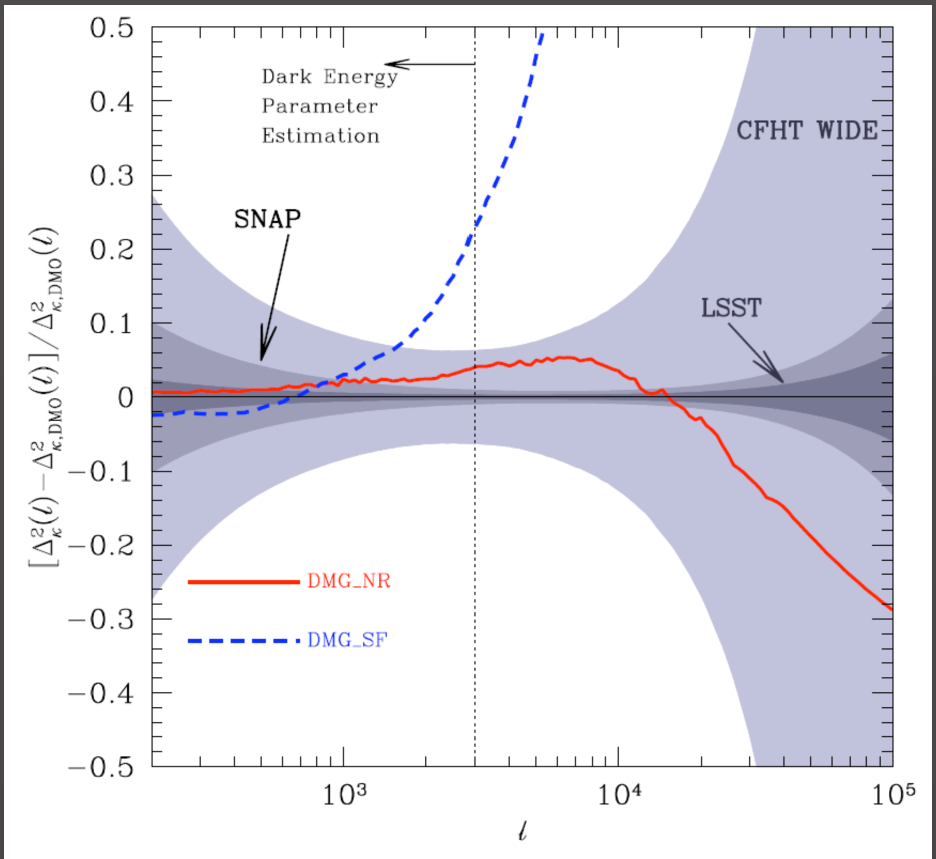

WL data can be used to self-calibrate baryon impact

Zentner, Rudd, Hu, Kravtsov

Weak Lensing & Photo-z Systematics

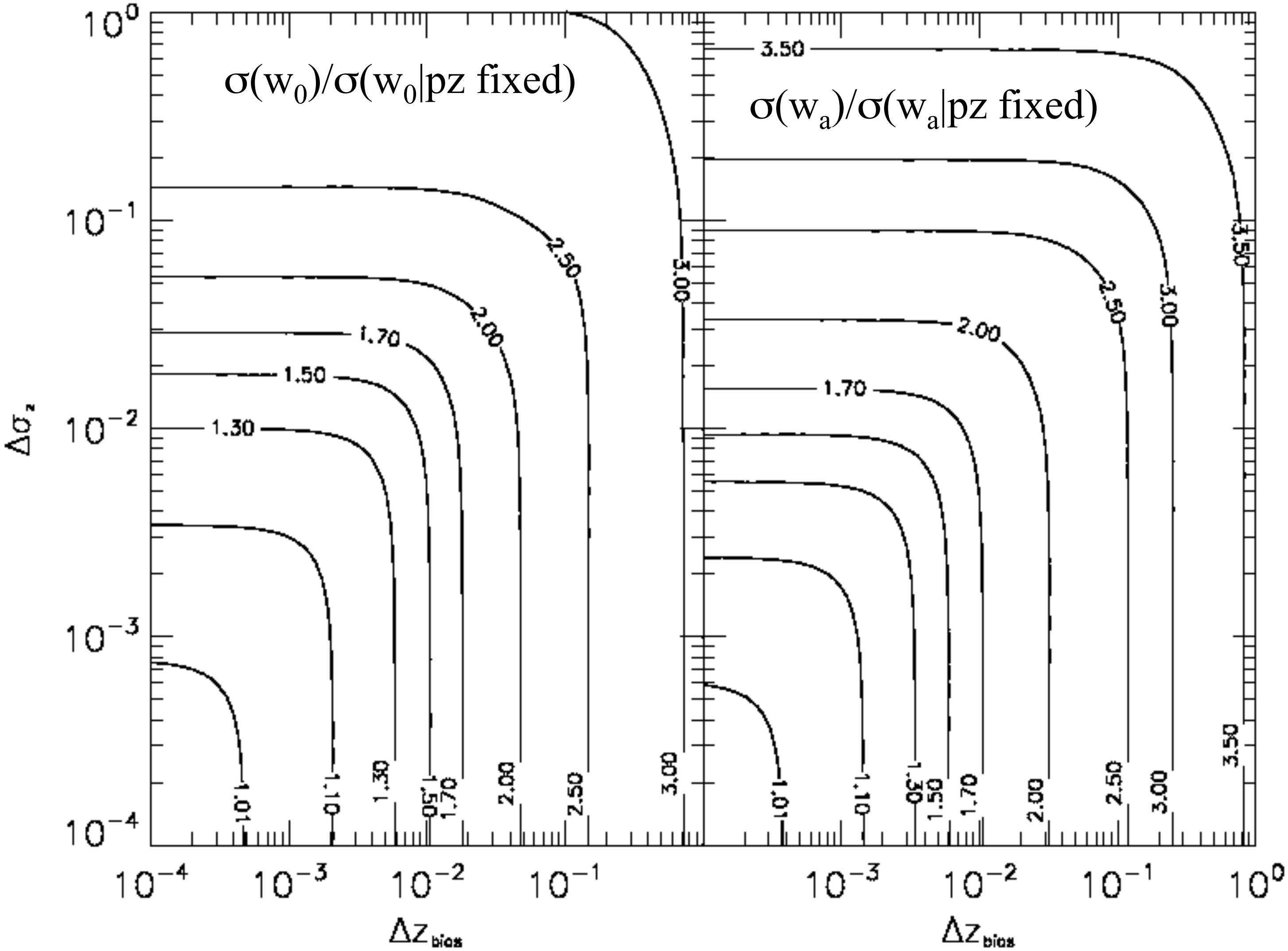

Ma

Weak Lensing Systematics: Anisotropic PSF

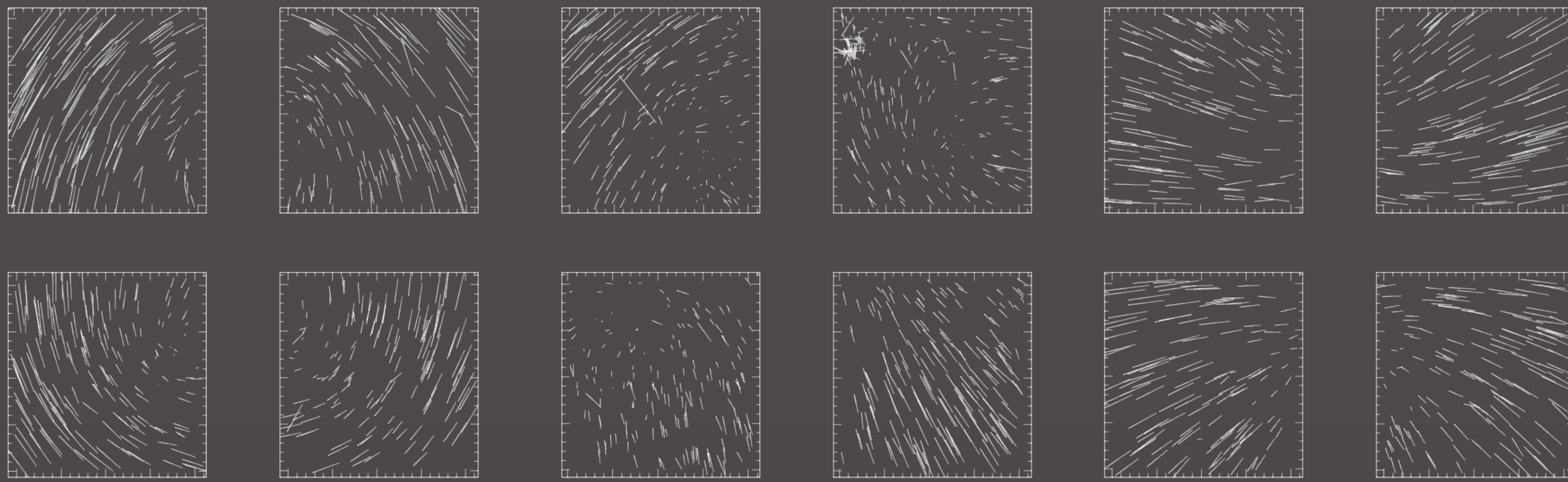

Focus too low — Focus (roughly) correct — Focus too high

- Whisker plots for three BTC camera exposures; ~10% ellipticity
- Left and right are most extreme variations, middle is more typical.
- Correlated variation in the different exposures: PCA analysis --> can use stars in all the images: much better PSF interpolation

Jarvis and Jain

PCA Analysis: Improved Systematics Reduction

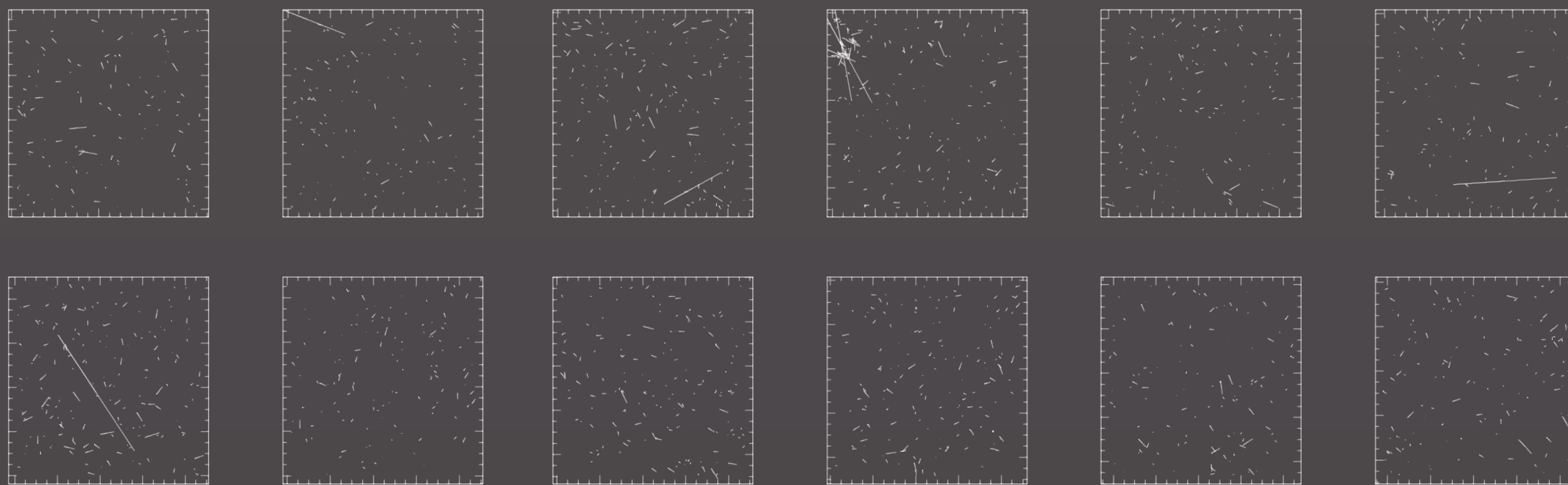

Focus too low   Focus (roughly) correct   Focus too high

- Remaining ellipticities are essentially uncorrelated.
- Measurement error is the cause of the residual shapes.
- 1st improvement: higher order polynomial means PSF accurate to smaller scales
- 2nd: Much lower correlated residuals on all scales!

Jarvis and Jain